INFLUENCE OF INFILL DENSITY AND NUMBER OF LAYERS ON MECHANICAL PROPERTIES OF 3D PRINTED PLA AND ABS SANDWICH STRUCTURES

UDC:655.36:620.1
Original scientific paper https://doi.org/10.46793/adeletters.2024.3.4.2

Mirko Karakašić[1*], Ivan Grgić[1], Vladimir Perak[1], Jure Marijić[1], Hrvoje Glavaš[2]

[1]University of Slavonski Brod, Mechanical Engineering Faculty in Slavonski Brod, Slavonski Brod, Croatia
[2]Josip Juraj Strossmayer University of Osijek, Faculty of Electrical Engineering, Computer Science and Information Technology, Osijek, Croatia

Abstract:
The increasing use of products manufactured by applying additive technologies encourages using materials with better mechanical properties. Depending on the type of material, its initial state, structure and mechanical properties, materials can be categorized differently. Combining polymer materials with different mechanical properties into composite structures makes it possible to obtain materials with better mechanical properties, which are then used on printers based on fused deposition modeling (FDM) 3D printing technology. This paper investigates the mechanical properties of samples made by combining Polylactic Acid (PLA) and Acrylonitrile Butadiene Styrene (ABS) polymer materials. The samples were produced with different proportions of the two materials regarding the number of layers and the infill density. The test was performed according to ISO 527 - 2: 2012 on a Shimadzu AGS-X 10 kN tensile test machine. For comparison, control samples of PLA and ABS materials were printed with 100% infill and showed the highest average force. Samples with a combination of materials did not produce the expected better results than samples made from one material. The reason for this is the occurrence of delamination of individual layers.

ARTICLE HISTORY
Received: 2 October 2024
Revised: 29 November 2024
Accepted: 19 December 2024
Published: 31 December 2024

KEYWORDS
Sandwich Structures, Additive Manufacturing, Fused Deposition Modeling, Polylactic Acid, Acrylonitrile Butadiene Styrene, Tensile Strength

1. INTRODUCTION

Additive manufacturing, particularly fused deposition modeling technology, has revolutionized the landscape of rapid prototyping and small-scale production.

The FDM process enables the production of complex geometric structures with a high degree of customization [1, 2], making it a desirable choice for various applications ranging from aerospace components [3] to medical implants. Polylactic Acid, a biodegradable and environmentally friendly thermoplastic polymer, is a commonly used material for FDM. However, the mechanical properties of FDM-printed PLA structures can be significantly influenced by various process parameters such as infill density, pattern, and print orientation. These parameters play a crucial role in determining the overall strength, durability and performance of the printed parts. Furthermore, the addition of ABS as infill to PLA has the potential to influence the overall mechanical performance of the printed structures. PLA-ABS sandwich structures produced using the Fused Deposition Modeling (FDM) technology of 3D printing have attracted a lot of attention in recent years due to their potential to combine the desirable properties of both materials [4]. These innovative structures typically consist of alternating layers of PLA and ABS, creating a sandwich structure with unique properties that could surpass the properties of the two materials individually. The tensile strength of

*CONTACT: Mirko Karakašić, e-mail: mkarakasic@unisb.hr

these sandwich structures is influenced by several critical factors, including the layer thickness, the infill density and the specific arrangement of the PLA and ABS layers within the structure. Incorporating ABS layers into these sandwich structures can significantly improve the composite's overall toughness and impact strength [5]. ABS is known for its high impact strength, durability and resistance to heat and chemicals, making it an excellent choice for improving the mechanical properties of the structure [6]. In addition, PLA contributes to better printability and dimensional stability due to its lower shrinkage rate and better layer adhesion during printing [2, 7]. This combination enables the production of parts with complex geometries and tight tolerances while maintaining structural integrity. However, interfacial adhesion between the PLA and ABS layers is a critical factor in the tensile strength of the composite. Weak interfacial adhesion can lead to delamination and premature failure under tensile loading and affect the overall performance of the sandwich structure. To overcome this challenge, the correct optimization of printing parameters is crucial, from aspect of surface quality [8]. Key factors to consider include each material's extrusion temperature, bed temperature, and cooling rate [9]. The extrusion temperature must be carefully controlled to ensure adequate flow and fusion of the polymer layers while preventing thermal degradation and delamination [10]. Similarly, the temperature of the print bed plays a crucial role in the adhesion between the first layer and the print bed and in maintaining constant thermal conditions throughout the printing process [11]. Techniques such as adjusting the layer height, optimizing the overlap between adjacent layers and performing post-treatments such as annealing or surface treatments can improve the adhesion between layers and the overall structural integrity. In addition, the design of the sandwich structure itself can also be optimized to maximize tensile strength [12, 13]. This can be seen in [14], where the authors use a dual extruder system to print PLA and ABS structures with the following parameters: layer thickness 0.1 mm, 0.2 mm and 0.3 mm, infill level 30%, 60% and 90% and infill patterns hexagon, triangle and 3D infill. They reported that using PLA and ABS together in the same 3D printed structure resulted in significantly higher tensile strength than using either material alone. Baca Lopez et al. [15] reported that the best sandwich-structured arrangement was the combination of outer skins of PLA and ABS cores, which had higher tensile strength, Young's modulus, and elongation at break compared to homogeneous materials. The test specimens consisted of 4 layers of each material, with 1.2 mm thick inner and outer cores. All specimens were printed with a rectilinear pattern. Brischetto et al. [16] have described the fabrication and mechanical behavior of 3D-printed sandwich structures using PLA and ABS polymers with classical and honeycomb cores with the following configurations. It was emphasized that the use of PLA for the outer skins leads to lower performances in Young's modulus due to the use of two different extruders. This resulted in poor adhesion between the skin and the core. Furthermore, the extruder changing process gives an early cooling of the previously printed layer, reducing the ability to completely adhere to the second layer. In addition, changing the extruder leads to premature cooling of the previously printed layer, which reduces its ability to fully adhere to the second layer. Some attempts were made to investigate the implementation of carbon fibers to show how to prevent delamination and deboning failures, which are presented in [17-19], and using the third material such as HIPS (High Impact Polystyrene) [20].

In this paper, the mechanical properties of the samples produced from the combination of the polymer materials PLA and ABS are analyzed to find out which mechanical properties can be achieved by simply using the standard 3D printing settings recommended by the manufacturer of the 3D printer. The same nozzle temperature was used for both materials. The grid pattern recommended by [21] and different infill densities and layer thicknesses were also used.

2. MATERIALS AND METHODS

The samples were divided into 8 batches of 10 samples each (Table 1). The density of the ABS and PLA materials and their infill percentage were varied. The first and second batches were control samples with an infill level of 100% and an equal proportion of ABS and PLA materials. In the third, fifth and seventh batches, the percentage of ABS infill was 25%; in the fourth, sixth and eighth batches, the percentage of ABS infill was 75%. In addition to the percentage of infill, the proportion of ABS material was also determined by the number of layers and their thickness. For example, one layer was printed in the third and fourth

batches, two layers in the fifth and sixth batches and three layers in the seventh and eighth batches. As the number of layers of ABS material increased, the proportion of PLA material also changed, at which the percentage of PLA material was kept at 100%.

Table 1. PLA and ABS proportions

No. of Batch	Material	Material Proportion, %		Infill, %		No. of ABS Layers	Mass, g	
		PLA	ABS	PLA	ABS	-	PLA	ABS
1	PLA	100	0	100	0	-	1.1	0
2	ABS	0	100	0	100		0	1
3	PLA, ABS	97.77	2.23	100	25	1	1.1	0.025
4	PLA, ABS	93.62	6.38	100	75		1.1	0.075
5	PLA, ABS	95.24	4.76	100	25	2	1	0.05
6	PLA, ABS	86.96	13.04	100	75		1	0.15
7	PLA, ABS	91.42	8.58	100	25	3	0.8	0.075
8	PLA, ABS	78.05	21.95	100	75		0.8	0.225

The infill pattern was set to Grid (Fig. 1.), which was selected via the Ulitmaker Cura Slicer software interface [22]. All samples were printed using the Wanhao Duplicator D12, D12/230 3D printer.

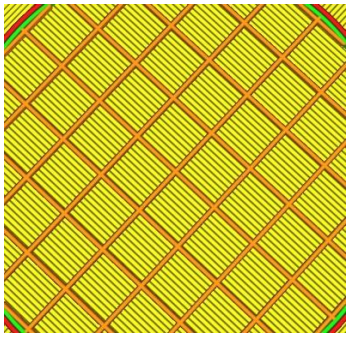

Fig. 1. Grid pattern

The samples were prepared in accordance with the ISO 527 - 2: 2012 standard. The geometry of the specimen is shown in Fig. 2 and the dimensions are in Table 2.

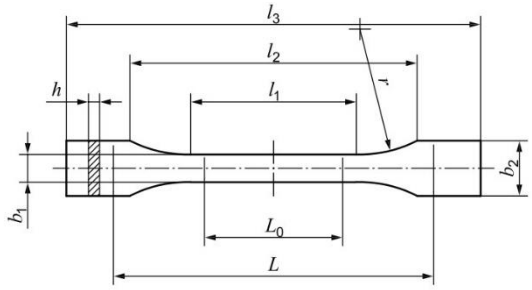

Fig. 2. Geometry of the specimen [6]

Table 2. Specimen dimensions according to ISO 527 - 2: 2012

Sample type	b_1, mm	b_2, mm	h, mm	l_1, mm	l_2, mm	l_3, mm	L, mm	L_0 mm	r, mm
1BA	5±0.5	10±0.5	≥2	30±0.5	58±2	≥75	$l_2\ ^{+2}_{0}$	25±0.5	≥30

2.1 CAD Modeling and 3D Printing

The Autodesk Inventor Professional 2023 software with the Educational license was used for this study. The CAD models of batches 1 and 2 were modeled as entire PLA and complete ABS specimens (Fig. 3). The height of the specimens was set to 2 mm, which is the minimum allowable height of the specimen, while the width was set to 5 mm. The CAD models for the specimens of batches 3 to 8 were modeled from multiple bodies, i.e. as sandwich structures.

In the Ultimaker Cura slicing software, the individual bodies were joined together to form one body. While they were still separate bodies, a suitable material was defined for each body. For batch 8, for example, the sandwich structure consists of 4 layers of PLA material (Fig. 4) and 3 layers of ABS material (Fig. 5) with different infill percentages with the thickness evenly distributed over the height of the sample (Fig. 6).

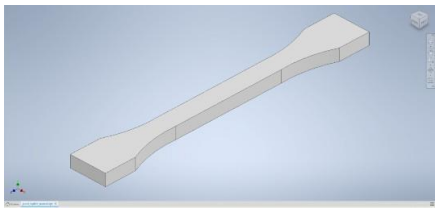

Fig. 3. Specimen body

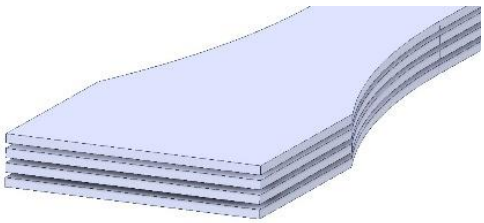

Fig. 4. PLA Layers

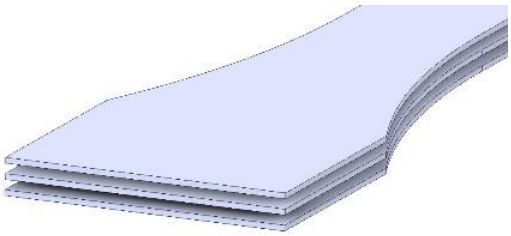

Fig. 5. ABS Layers

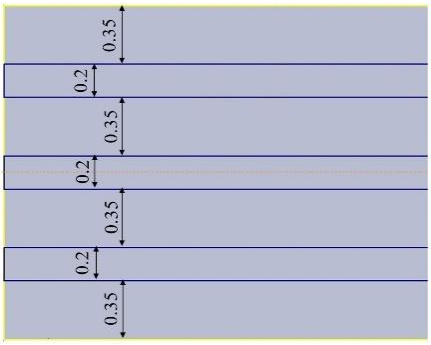

Fig. 6. Thickness distribution

The horizontal position of the samples on the build plate was selected for 3D printing (Fig. 7). The grid pattern and the 25% infill are shown in Fig. 8 and 75% in Fig. 9. The PLA material is labeled brown and the ABS material green. The examples of the sandwich structures are shown in Fig. 10. The 3D printing parameters are listed below in Table 3, and the process of 3D printing is shown in Fig. 11.

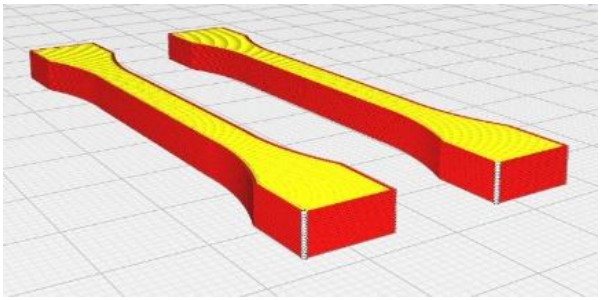

Fig. 7. Horizontal position for 3D printing

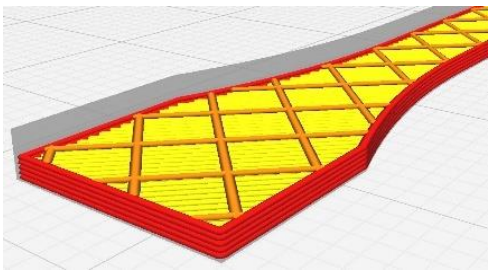

Fig. 8. 25% ABS grid pattern

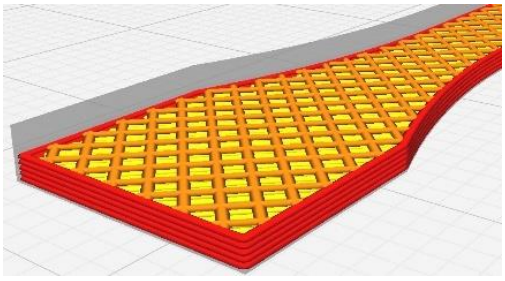

Fig. 9. 75% ABS grid pattern

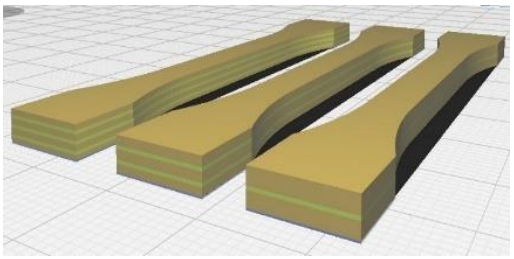

Fig. 10. PLA-ABS sandwich structures

Table 3. General parameters of the 3D printing process

Parameter	Units	Value
Temperature	°C	230
Bed temperature	°C	45
Layer height	mm	0.2
Diameter	mm	1.75
Printing Speed	mm/s	50
Layer Orientation	°	±45
Number of perimeters		1
Nozzle diameter	mm	0.4

Fig. 11. 3D Printing

3. RESULTS AND DISCUSSION

The mechanical properties were determined using a Shimadzu AGS-X 10 kN device [23], (Fig. 12). The specimens were continuously loaded until failure occurred. The test speed was 2 mm/min. The following variables were analyzed: maximum force at failure point and tensile strength. Failure occurred in all samples within the measurement range. The example is shown in Fig. 13. The results of the mechanical properties are listed in Table 4 to Table 11. The Force-Stroke diagrams for batch 3 to batch 8 are shown in Fig. 14 to Fig. 19. Delamination of the layers occurred in four specimens during the test, but this had no influence on the final result.

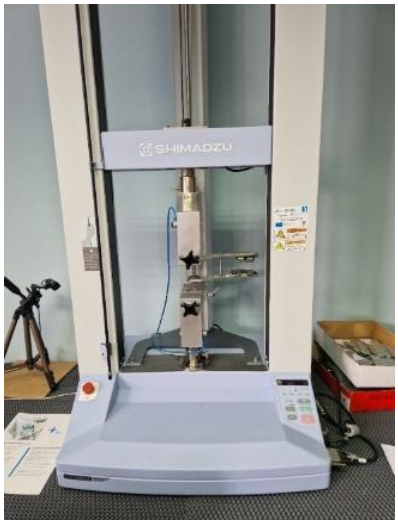

Fig. 12. Shimadzu AGS-X 10 kN machine

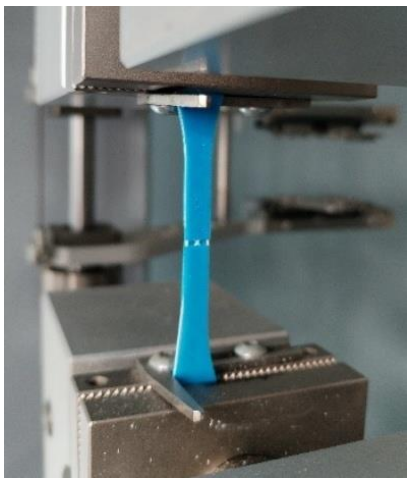

Fig. 13. The specimen failure

Table 4. Results of the batch 1

Specimen number	Batch	Max. Force, N	Tensile Strength, MPa
1.	1	466.46	46.64
2.	1	458.32	45.83
3.	1	451.43	45.14
4.	1	448.06	44.80
5.	1	458.13	45.81
6.	1	430.79	43.07
7.	1	428.95	42.89
8.	1	427.70	42.77
9.	1	442.17	44.21
10.	1	443.31	44.33
	Average value	445.53	44.55

Table 5. Results of the batch 2

Specimen number	Batch	Max. Force, N	Tensile Strength, MPa
1.	2	351.40	35.14
2.	2	385.36	38.36
3.	2	349.18	34.91
4.	2	341.67	34.16
5.	2	350.31	35.03
6.	2	377.25	37.72
7.	2	344.34	34.43
8.	2	354.78	35.47
9.	2	371.88	37.18
10.	2	357.88	35.78
	Average value	354.76	35.47

Table 6. Results of the batch 3

Specimen number	Batch	Max. Force, N	Tensile Strength, MPa
1.	3	281.22	28.12
2.	3	290.28	29.02
3.	3	287.29	28.72
4.	3	302.93	30.29
5.	3	286.44	28.64
6.	3	287.11	28.71
7.	3	297.01	29.70
8.	3	287.29	28.72
9.	3	294.39	29.43
10.	3	287.12	28.71
	Average value	288.67	28.86

Table 7. Results of the batch 4

Specimen number	Batch	Max. Force, N	Tensile Strength, MPa
1.	4	304.62	30.46
2.	4	289.68	28.97
3.	4	292.91	29.29
4.	4	296.06	29.61
5.	4	300.44	30.04
6.	4	282.21	28.22
7.	4	282.37	28.24
8.	4	292.58	29.26
9.	4	282.79	28.28
10.	4	296.06	29.61
	Average value	291.97	29.20

Table 8. Results of the batch 5

Specimen number	Batch	Max. Force, N	Tensile Strength, MPa
1.	5	178.98	17.90
2.	5	185.55	18.55
3.	5	193.18	19.32
4.	5	197.80	19.78
5.	5	198.03	19.80
6.	5	181.33	18.13
7.	5	193.30	19.33
8.	5	193.52	19.35
9.	5	193.99	19.40
10.	5	187.70	18.77
	Average value	190.34	19.03

Table 9. Results of the batch 6

Specimen number	Batch	Max. Force, N	Tensile Strength, MPa
1.	6	208.89	20.89
2.	6	222.00	22.20
3.	6	231.92	23.19
4.	6	204.53	20.45
5.	6	241.19	24.12
6.	6	214.99	21.50
7.	6	216.67	21.67
8.	6	235.38	23.54
9.	6	223.64	22.36
10.	6	227.96	22.80
	Average value	222.72	22.27

Table 10. Results of the batch 7

Specimen number	Batch	Max. Force, N	Tensile Strength, MPa
1.	7	205.87	20.59
2.	7	195.72	19.57
3.	7	217.00	21.70
4.	7	217.12	21.71
5.	7	217.38	21.74
6.	7	211.78	21.18
7.	7	213.06	21.31
8.	7	208.53	20.85
9.	7	208.86	20.89
10.	7	197.63	19.76
	Average value	209.30	20.93

Table 11. Results of the batch 8

Specimen number	Batch	Max. Force, N	Tensile Strength, MPa
1.	8	221.42	22.14
2.	8	246.61	24.66
3.	8	269.50	26.95
4.	8	272.43	27.24
5.	8	275.54	27.55
6.	8	256.29	25.63
7.	8	256.11	25.61
8.	8	241.21	24.12
9.	8	249.75	24.97
10.	8	258.90	25.89
	Average value	254.78	25.48

Two-way ANOVA statistical analysis without repeated measures was used; we have different conditions in each combination of factor levels. First, it was necessary to test assumptions such as a test of variance equality using Levene's test (Table 12) and normal distribution of measured tensile strength for each sample size using Kolmogorov-Smirnov's test (Fig. 20). Results of ANOVA statistics are presented in Table 13.

The statistical analysis showed a significant difference between the groups of the independent variable No. of ABS layers in relation to the dependent variable Tensile Strength, $p < 0.001$, that there is a significant difference between the groups of the independent variable ABS Infill in relation to the dependent variable Tensile Strength, $p < 0.001$ and that there is an interaction between the two variables No. of ABS layers and ABS Infill in relation to the dependent variable Tensile Strength, $p < 0.001$.

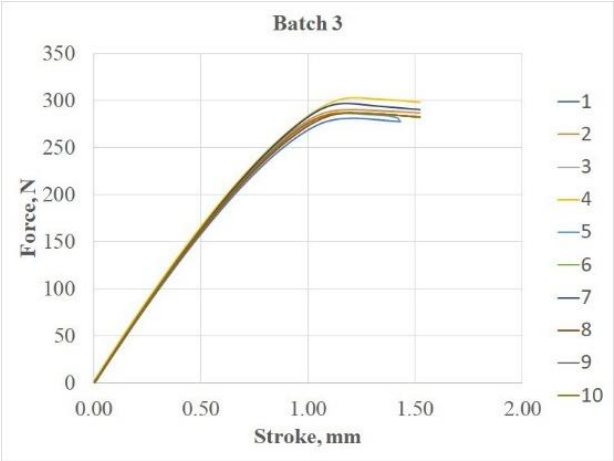

Fig. 14. Force-Stroke for batch 3

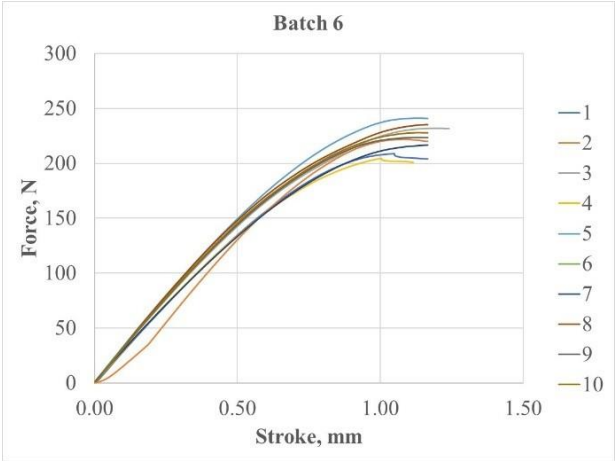

Fig. 17. Force-Stroke for batch 6

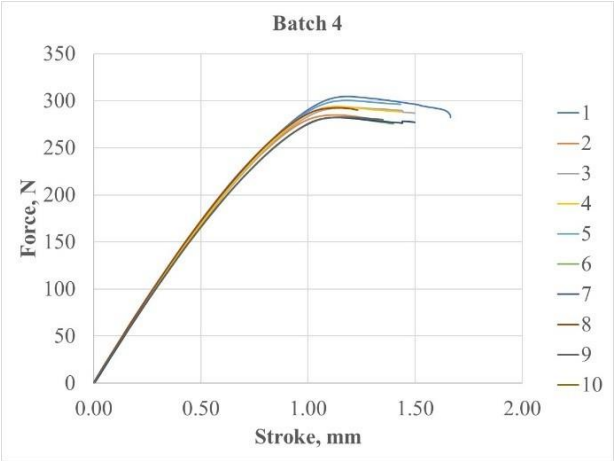

Fig. 15. Force-Stroke for batch 4

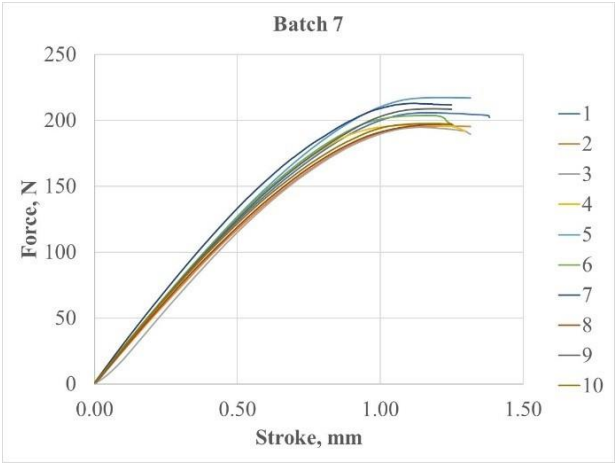

Fig. 18. Force-Stroke for batch 7

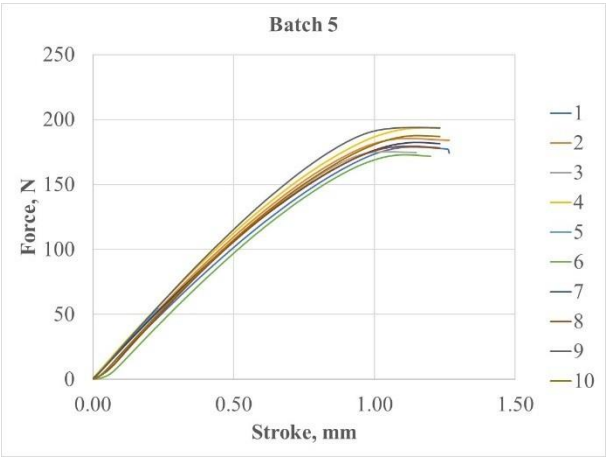

Fig. 16. Force-Stroke for batch 5

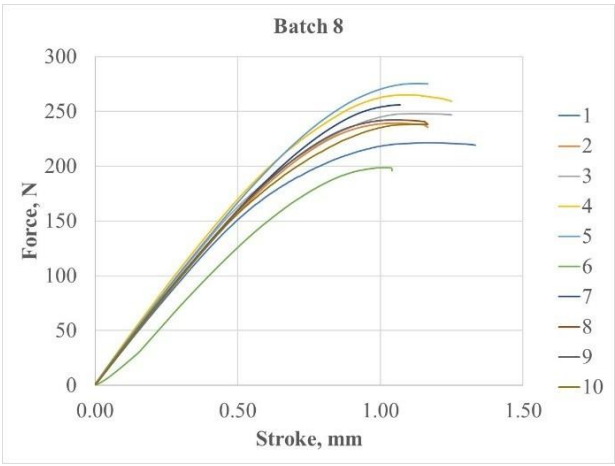

Fig. 19. Force-Stroke for batch 8

Table 12. Levene's test of variance equality

Test	F	df_1	df_2	p
Levene's Test (Mean)	2.25	5	54	0.062

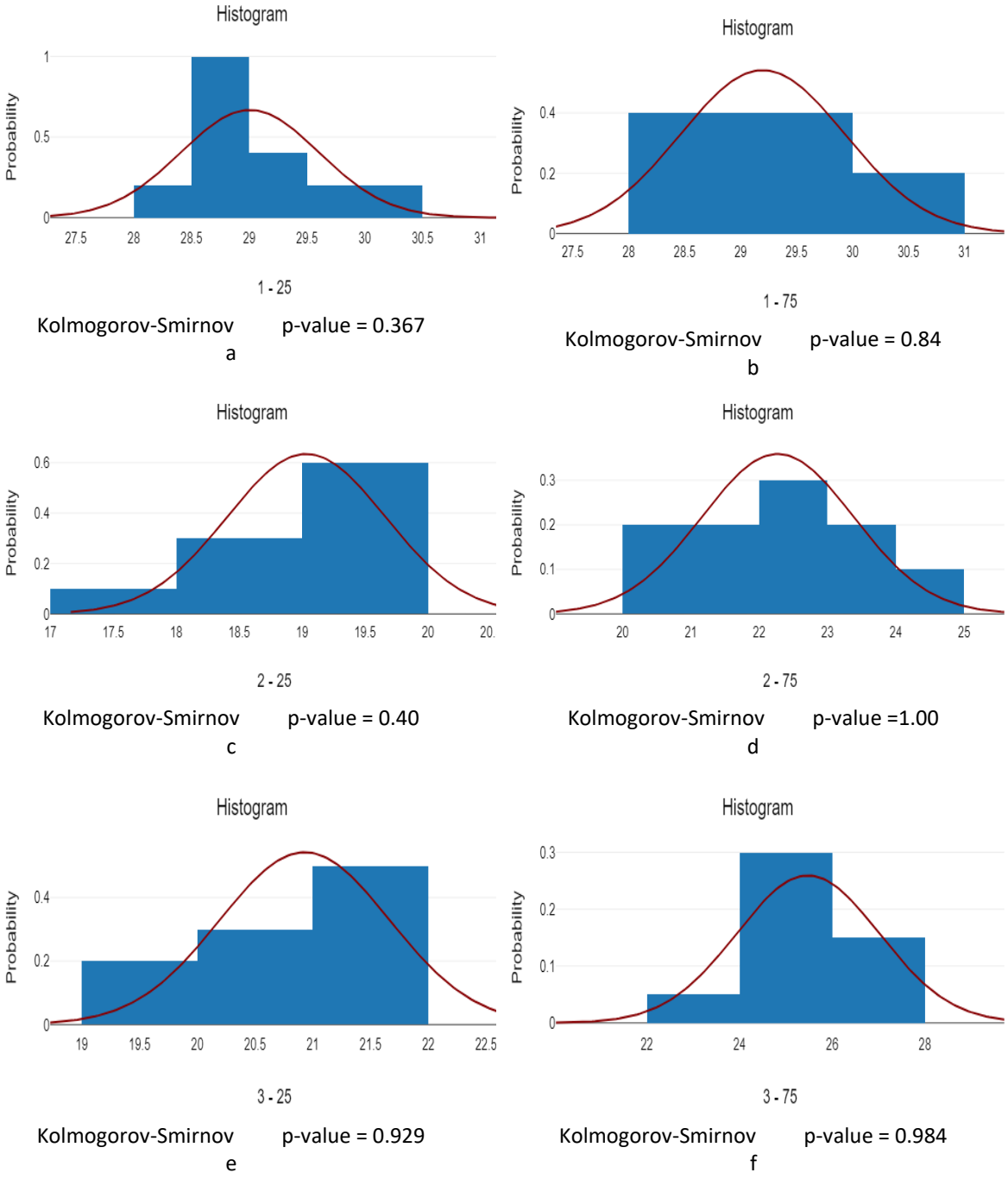

Fig. 20. Normal distributions of the Tensile Strength per sample

Table 13. ANOVA statistics

	Type III Sum of Squares	df	Mean Squares	F	p	η^2_p
No. of ABS layers	751.32	2	375.66	373	<0.001	0.93
ABS Infill, %	106.05	1	106.05	105.3	<0.001	0.66
No. of ABS layers x ABS Infill, %	49.92	2	24.96	24.78	<0.001	0.48
Error	54.38	54	1.01			

4. CONCLUSION

A total of 80 samples were tested. Since the mechanical properties of PLA and ABS materials are already well-known, the obtained properties are shown just with tables but without the presentation of diagrams for the correlation with proposed sandwich structures. However, the mechanical properties of 60 samples are presented and statistically analyzed with tables and diagrams. The results showed that the combination of PLA and ABS did not lead to better mechanical properties of the material than either material on its own. During the test, some samples showed delamination between the layers, which became more pronounced as the number of layers of ABS material increased. The samples with 25% ABS infill had poorer mechanical properties than those with 75% ABS infill. It can be concluded that general settings for 3D printing are not recommended for such sandwich structures, which is also confirmed by the studies published so far. There is still a need to find optimal parameters considering what these structures are trying to achieve.

There is a significant difference between the variables tested, so valid parameter optimization is required for this type of study.

In summary, PLA-ABS sandwich structures represent an innovative approach to utilizing the strengths of both materials in FDM 3D printing applications. By carefully optimizing the printing parameters, improving interfacial adhesion and using advanced design strategies, it is possible to maximize the tensile strength of these composites and exploit the synergistic effects of both materials. Our future research will be based on the integration of ABS material into the PLA layer so that two materials are present simultaneously in one layer.

NOTE

This paper is the result of a Master's thesis by student Vladimir Perak under the mentorship of Ph.D. Mirko Karakašić, Full Professor and co-mentorship of Ph.D. Ivan Grgić, Assistant Professor.

Conflicts of Interest

The authors declare no conflict of interest.

REFERENCES

[1] A. Waleed, A. Sidra, A. Fady, Z. Essam, Mechanical performance of three-dimensional printed sandwich composite with a high-flexible core. *Proceedings of the Institution of Mechanical Engineers, Part L: Journal of Materials: Design and Applications*, 235(6), 2021: 1382-1400. https://doi.org/10.1177/14644207211011729

[2] H. Junaedi, M.A. Abd El-baky, M.M. Awd Allah, T.A. Sebaey, Mechanical Characteristics of Sandwich Structures with 3D-Printed Bio-Inspired Gyroid Structure Core and Carbon Fiber-Reinforced Polymer Laminate Face-Sheet. *Polymers*, 16(12), 2024: 1698. https://doi.org/10.3390/polym16121698

[3] K. Sugiyama, R. Matsuzaki, M. Ueda, A. Todoroki, Y. Hirano, 3D printing of composite sandwich structures using continuous carbon fiber and fiber tension. *Composites Part A: Applied Science and Manufacturing*, 113, 2018: 114-121. https://doi.org/10.1016/j.compositesa.2018.07.029

[4] P.K. Patro, S. Kandregula, M.N. Suhail Khan, S. Das, Investigation of mechanical properties of 3D printed sandwich structures using PLA and ABS. *Materials Today Proceedings*, 2023. https://doi.org/10.1016/j.matpr.2023.08.366

[5] A. Galatas, H. Hassanin, Y. Zweiri, L. Seneviratne, Additive Manufactured Sandwich Composite/ABS Parts for Unmanned Aerial Vehicle Applications. *Polymers*, 10(11), 2018: 1262. https://doi.org/10.3390/polym10111262

[6] V. Perak, Structural optimization and mechanical properties of composite materials made by FDM 3D printing technology, Master thesis. *University of Slavonski Brod, Mechanical Engineering Faculty*, Slavonski Brod, Croatia, 2024.

[7] M. Johar, A.A. Rosli, R.K. Shuib, Z.A.A. Hamid, M. K. Abdullah, K.M.K. Ishak, A. Rusli, Dimensional stability of poly (lactic acid) (PLA) parts fabricated using fused deposition modelling (FDM). *Progress in Rubber, Plastics and Recycling Technology*, 0(0), 2024: 14777606241262882. https://doi.org/10.1177/14777606241262882

[8] S. Djurović, D. Lazarević, B. Ćirković, M. Mišić, M. Ivković, B. Stojčetković, M. Petković, A. Ašonja, Modeling and Prediction of Surface Roughness in Hybrid Manufacturing – Milling after FDM Using Artificial Neural Networks. *Applied Sciences*, 14(14), 2024: 5980. https://doi.org/10.3390/app14145980

[9] K. Kalia, A. Ameli, Interfacial Bond Strength of Various Rigid / Soft Multi-Materials Printed via

Fused Filament Fabrication Process. *Proceedings of the ASME 2020 Conference on Smart Materials, Adaptive Structures and Intelligent Systems. ASME 2020 Conference on Smart Materials, Adaptive Structures and Intelligent Systems*, 2020: V001T01A010. https://doi.org/10.1115/SMASIS2020-2298

[10] S. Li, K. Wang, J.P.M. Correia, Y. Liu, S. Ahzi, Investigating gradient temperature control for enhanced interfacial bonding behavior in material extrusion 3D printing continuous fiber reinforced polymer composites. *European Journal of Mechanics - A/Solids*, 107, 2024: 105349. https://doi.org/10.1016/j.euromechsol.2024.105349

[11] M. Spoerk, J. Gonzalez-Gutierrez, J. Sapkota, S. Schuschnigg, C. Holzer, Effect of the printing bed temperature on the adhesion of parts produced by fused filament fabrication. *Plastics, Rubber and Composites*, 47(1), 2018: 17-24. https://doi.org/10.1080/14658011.2017.1399531

[12] P.M. Raghava, G.J. Chandra Reddy, 3D-Printed lightweight sandwich structures with carbon – fibre - reinforced polymer skins and glass - fibre - reinforced polymer core: a comparative study. *Smart Materials & Methods*, 2024: 1-19. https://doi.org/10.1080/29963176.2024.2434868

[13] Q. Estrada, J. Zubrzycki, E. Reynoso-Jardon, D. Szwedowicz, A. Rodriguez-Mendez, M. Marchewka, J. Vergara-Vazquez, A. Bastarrachea, J. Silva, Numerical Study of the Energy Absorption Performance of 3D Printed Sandwich Structures. *Advances in Science and Technology Research Journal*, 17(5), 2023: 153-162. https://doi.org/10.12913/22998624/171496

[14] B. Yermurat, Ö. Seçgin, V. Taşdemir, Multi-material additive manufacturing: investigation of the combined use of ABS and PLA in the same structure. *Materials Testing*, 65(7), 2023: 1119-1126. https://doi.org/10.1515/mt-2022-0368

[15] D.M. Baca Lopez, R. Ahmad, Tensile Mechanical Behaviour of Multi-Polymer Sandwich Structures via Fused Deposition Modelling. *Polymers*, 12(3), 2020: 651. https://doi.org/10.3390/polym12030651

[16] S. Brischetto, C.G. Ferro, R. Torre, P. Maggiore, 3D FDM production and mechanical behavior of polymeric sandwich specimens embedding classical and honeycomb cores. *Curved and Layered Structures*, 5(1), 2018: 80-94. https://doi.org/10.1515/cls-2018-0007

[17] S. Vellaisamy, R. Munusamy, Experimental study of 3D printed carbon fibre sandwich structures for lightweight applications. *Defence Technology*, 36, 2024: 71-77. https://doi.org/10.1016/j.dt.2023.11.019

[18] S.W. Ahmed, G. Hussain, K. Altaf, S. Ali, M. Alkahtani, M.H. Abidi, A. Alzabidi, On the Effects of Process Parameters and Optimization of Interlaminate Bond Strength in 3D Printed ABS / CF-PLA Composite. *Polymers*, 12(9), 2020: 2155. https://doi.org/10.3390/polym12092155

[19] S.W. Ahmed, G. Hussain, K.A. Al-Ghamdi, K. Altaf, Mechanical properties of an additive manufactured CF-PLA / ABS hybrid composite sheet. *Journal of Thermoplastic Composite Materials*, 34(11), 2021: 1577-1596. https://doi.org/10.1177/0892705719869407

[20] A. Suresh, P.S. Dadi, T. Tamilvizhi, P.P. Keerthana, R. Surendran, Numerical analysis of compression test on 3D printed reinforced ABS and PLA. *IET Conference Proceedings*, 2023(44), 2024: 544-549. https://doi.org/10.1049/icp.2024.0993

[21] A. Pandzic, D. Hodzic, Tensile Mechanical Properties Comparation of PETG, ASA and PLA-Strongman FDM Printed Materials With and Without Infill Structure. *Proceedings of the 33rd International DAAAM Virtual Symposium ''Intelligent Manufacturing & Automation''*, October 27-28, 2022, Hosted from Vienna University of Technology, Vienna, Austria, pp.0221–0230. https://doi.org/10.2507/33rd.daaam.proceedings.031

[22] UltiMaker, 'Cura 5.1.1 3D printing software', 5.1.1. https://ultimaker.com/software/ultimaker-cura (Accessed: March 10, 2023.)

[23] Shimadzu Excellence in Science, AGS – X Universal Testing Machines with Convincing Cost Performance. https://shimadzu-testing.com/en/products/universal-testing-machines/ags-x/ (Accessed: October 1, 2024).